A SOLAR AND VECTOR CLASS FOR THE OPTICAL SIMULATION OF SOLAR CONCENTRATING SYSTEMS

Damien Buie and Anne Gerd Imenes,
Solar Energy Group, School of Physics, Building A28 University of Sydney, Australia,
Ph: +61 (0)2 93515979, Fax: +61 (0)2 93517725, email: buie@physics.usyd.edu.au

Abstract - This paper provides a tool to simulate dynamic abstract solar concentrators that can easily be utilised to optimise the optics and hence designs of solar power systems that is freely available. Two libraries of functions written in the computer language c++ are used in this paper to provide this infrastructure. The first library *solar.h* generates the terrestrial solar beam and consists of four main parts: the PSA Algorithm for calculating the solar vector, SPECTRAL2 simulating the spectral energy distribution and two new computer codes that describe the spatial energy distribution of the solar image and the broadening that occurs when a solar image is reflected off a non-ideal mirrored surface. The second library *vector.h* is a standard vector class that includes intrinsic functions in vector algebra that facilitate a simple ray-tracing algorithm. The combination of these two libraries allows simple and complex structures to be generated and modelled, and effective comparisons between various designs of solar concentrators carried out. This paper then goes on to provide implementation of the algorithms for solar energy applications.

1. INTRODUCTION

The Solar Research Group within the School of Physics at the University of Sydney is primarily concerned with the creation of large-scale (modular) solar power systems. With the growing cost of experimental research within this field and the requirement to achieve the peak performance from such systems, so as to compete against more established forms of power generation, computational modelling is an ideal method to carry out this research at an affordable cost.

Presently, there are a large number of computer resources, freely available, that have been created to model both individual components as well as entire systems, for solar power applications (Blanco-Muriel and Alarcon-Padilla, 2000; Blanco-Muriel et al., 2001; Myers et al., 2002). Generally, these resources vary in their structure, programming language, and relevance to a specific task, which hinders their usability for broader applications. Going further, reproducibility, which is essential in scientific research is hindered, as the operating parameters of one or more of the pieces of computer code, used in modelling, are not always made publicly available.

The purpose of this paper is to provide the basic tools to generate complex structures. To achieve this, the optics were divided into a number of components: the most obvious of these is the geometry of the optical system and its orientation relative to the sun. Of equal importance is the spatial and spectral distribution of the terrestrial solar beam, due to the dynamic nature of the atmosphere, and finally, considering concentrating systems, the effect to the beam of reflecting it off a non-ideal mirrored surface.

This information is presented in two libraries of functions (classes written in the computer language c++). The first *solar.h* contains an abstract representation of the terrestrial solar beam, including the systemic effect of reflecting that beam off a non-ideal mirrored surface. The second *vector.h*, creates the basis of Euclidean space, together with functions that can facilitate a simple ray-tracing algorithm.

Within this framework complex structures can be generated, and, assuming all of these components are modelled representing real systems, then a good understanding of the optical performance can be gained. It needs to be pointed out that the fundamental computer codes and algorithms described in this work do not specifically simulate a particular solar energy conversion system, whether it is a dish system or a central receiver. More so, it provide the infrastructure to facilitate the creation of any such system, in which the solar input parameters that clearly describe the reflected terrestrial beam are common, facilitating reproducibility.

This paper is divided in three parts. The first describes the principle components required to create an abstract solar image reflected off a mirrored surface and the functions that generate them. The second provides an analysis of a simple ray-tracing framework to facilitate high-resolution optical maps for simulating the absorber plane of concentrating systems. Thirdly, the flux distributions for a range of concentrating systems have been generated to illustrate the versatility of the code. Those simulated are: a trough collector, a linear Fresnel system, a Fresnel dish concentrator and a central tower receiver. As the solar distribution is common to all of the systems, a direct comparison of the systems is also justifiable.

2. THE SOLAR CLASS

Three components are required to create an abstract model of the terrestrial solar beam: the position of the sun

in the sky, its spectral and spatial energy distribution and the broadening of the spatial energy distribution after its reflection off a non-ideal mirrored surface. Combined these components completely characterises the reflected beam.

2.1 Spatial energy distribution

As solar radiation travels from the near vacuum of space to the terrestrial Earth, it must pass through the Earth's atmosphere. Where the solar radiation interacts with large particles in the atmosphere (Mie, 1908; Junge, 1963), forward scattering of the direct beam occurs transferring some part of the solar radiation from within the confines of the solar disc, to the circumsolar region (solar aureola). The resulting radial spatial energy distribution (sunshape) created from the combination of atmospheric scattering and limb darkening of the solar source affects the resulting energy distribution in the absorber plane of solar concentrators.

The Lawrence Berkley Laboratories began investigating terrestrial sunshapes in the mid to late 1970s and early 1980s. They compiled a large number of radial solar profiles, representing the spatial energy distribution of the sun (Noring et al., 1991), into what is called the reduced database (RDB). Following this research, significant contributions by a number of authors (described in Buie et al. 2003) led to both quantifying the degree to which the amount of energy in the circumsolar region of the sky effected solar concentrators and illustrated trends that were present in sunshapes at various locations.

More recently, Buie and Monger (2001) and Neumann et al. (2002) independently inferred that the spatial energy distribution of the sun, if represented by its circumsolar ratio (CSR), illustrated, on average, invariance to a change in location for all of the sites where data had been collected. The CSR (χ) is defined as the radiant flux contained within the circumsolar region of the sky (Φ_{cs}), divided by the incident radiant flux (Φ_i) from the direct beam and aureole,

$$\chi = \frac{\Phi_{cs}}{\Phi_i} . \qquad [1]$$

Buie et al. (2003) went further, defining an algorithm that could be used to describe the sunshape:

$$\phi(\theta) = \begin{cases} \dfrac{\cos(0.326\theta)}{\cos(0.308\theta)} & \text{for } \{\theta \in \Re \mid \ 0 < \theta < 4.65\} \\ e^{\kappa}\theta^{\gamma} & \text{for } \{\theta \in \Re \mid 4.65 < \theta < 44\} \end{cases}, \qquad [2]$$

where κ and γ are give by,

$$\begin{aligned} \kappa &= 0.9\ln(13.5\chi)\chi^{-0.3} \\ \gamma &= 2.2\ln(0.52\chi)\chi^{0.43} - 0.1 \end{aligned} , \qquad [3]$$

and χ is again the circumsolar ratio of the solar distribution and θ is measured in milliradians. This algorithm has a strong correlation with these observed data. The algorithm is invariant to changes in geographic location when representing averaged observed solar profiles, and can be used as a generic sunshape model based upon the circumsolar ratio.

Within the solar class the spatial solar energy distribution of the direct beam and circumsolar region is simulated by a solar image. The image is created by an array of appropriately weighted vectors. Each vector defines a point on that image. The vectors are arranged on a surface, such that they define an angular displacement from the solar vector (θ_i) along a series of limbs (Figure 1) forming a wagon wheel. The resulting voxel (a vector describing each point on a surface) represents its corresponding segment of an arc. Combined it creates a solar image with a total weight of 1, extending to an angular displacement of 43.6 mrad (default) from the solar vector (defined in Section 2.3). The default values for the dependent variables are given in Table 1

Function	Variable	Default	Units
definecsr	circumsolar ratio	0.05	
definesigma	stddev mirror error	3.5	mrad
definesunlimit	disk limit, csr limit	4.65 43.6	mrad mrad
defineNumPoints	No. spurs no.radial po	100 50	integer integer

Table 1: Default variable for the spatial energy distribution of the solar image.

2.2 Reflection off a mirrored surface

If the terrestrial solar image were reflected off a perfect (planar) surface, the reflected image would be identical to the original. However in real systems, the reflection of an image off a surface causes a distortion in that image. Two principle effects cause this distortion in solar concentrators. Firstly, real surfaces interact with the reflected radiation, causing the expected specula reflection to form a dispersive cloud. Secondly, mirror shapes are not perfect, that is to say, the variations in the surface normals from the ideal mirror shape are an additional influence on the reflected image.

Johnston (1995) showed that by considering as a systemic mass, both the slope error (defined as the angular deviation of the actual surface normal vectors from their ideal directions, measured in milliradians (Johnston, 1998)) and surface dispersion effects, the combined error could be treated by the probability distribution (P),

$$\frac{dP}{d\theta} = \frac{\theta}{\sigma^2} e^{-\theta^2/2\sigma^2} , \qquad [4]$$

where σ is the standard deviation of the combined surface slope and dispersion error, and θ is the radial displacement of a reflected beam from the specula direction. A real surface can then be characterised by the standard deviation of the probability distribution. As an example of different surfaces, a high quality optical mirror has a probability distribution with a standard deviation of about 0.2 mrad, whereas poorer quality solar reflectors could have a standard deviation as high as 8 mrad.

Mirror alignment and tracking errors are further significant sources of error in predicting the resultant flux distribution in solar concentrators. It is only when a statistically significant number of mirrors or a long time average is considered, that a distribution in tracking error can be modelled by a radial Gaussian distribution (Bendt et al., 1979). If either of these criteria is met, the standard deviation of the alignment and tracking error can be simply added to the standard deviation of the combined surface slope and dispersion error. Movement in the absorber from the ideal position could be treated in the same manner.

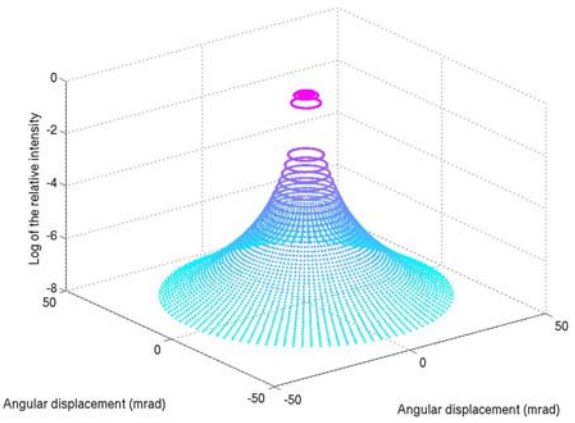

Figure 1: Representation of a reflected terrestrial solar beam consisting of 100 radial limbs of 50 points each.

Simulating the solar image reflected of a mirrored surface can be performed by the convolution of the solar image and a two dimensional representation of the radial Gaussian distribution in Equation 4. It must be pointed out that the convolution of a radial error distribution and a solar image is only truly representative of a reflected beam at normal incidents (Rabl, 1985). For non-normal reflection, being the majority of reflections the error distribution would be asymmetric (or elliptical). Therefore this method is only an approximation of a real system. To circumvent this process the solar image can be left with a standard deviation of errors of zero, and the error distribution in the surface normals (being primarily responsible for the error) can be build into the shape of the mirror module.

2.3 The PSA Algorithm

Solar tracking systems require a precise knowledge of the local horizontal coordinates of the sun. Blanco-Muriel et al. (2001) examined the accuracy of several computer codes used to predict this angle: the corrected Walraven (1978,1979) algorithm, the Michalsky (1988) algorithm, along with some more simplified models, and stated that the average deviation from the true solar vector (the unit vector describing the position of the sun in the sky from a given location) was 0.271 and 0.207 minutes of arc respectively.

Blanco-Muriel et al. (2001) wrote that, "*Even though the Michalsky algorithm may be considered good enough for most solar tracking applications, its accuracy, computing efficiency, and ease of use can still be improved.*" The algorithm they proposed, the PSA Algorithm, has advanced memory management, greater speed and robustness and an average deviation from the solar vector of 0.147 minutes of arc. The PSA Algorithm is presently used as an open loop tracking system for the EuroTrough direct steam line at the Plataforma Solar de Almeria (PSA).

Because of the PSA Algorithm's accuracy, it was included within the solar class to calculate the position of the solar vector. (The code can be downloaded from http://www.psa.es/sdg/sunpos.htm). Apart from the reallocation of variables, one small modification was made to the code to include the calculation of the day number that is required to generate the spectral solar energy distribution. The default variables declared during the initiation of the solar class with regards to calculating the solar vector are for the location of Sydney, Australia (Longitude 151.2^{o}, Latitude -33.867^{o}) on the 1st of January 2000, at 12:06 +11 Universal Time.

2.4 The spectral energy distribution

The atmosphere acts as an active absorber, re-emitter and small angle scatterer of solar radiation. As each of these processes is wavelength specific, the resulting terrestrial solar spectrum is dependent on both the constituents of the atmospheric profile and the optical path length of the radiation. As the performance of most solar power systems is spectrally dependent, in order to simulate the optical performance the spectral characteristics of the terrestrial radiation must be determined.

The spectral composition of solar radiation is pertinent to photovoltaics as well as for solar thermal applications. The absorption characteristics of selective surfaces, transmission of light through an absorber windows and reflection of sunlight off metal coated mirrors are common to all solar concentrators and are spectrally dependent.

There are presently three accepted methods for generating the terrestrial solar spectrum (Myers et al., 2002). Line-by-line models, Band models and "simpler models", based on the parameterisations of transmittance and absorption functions, for the basic atmospheric

constituents; ordered according to decreasing accuracy and subsequently decreasing computation time.

For the purpose of establishing a comprehensive computational tool, speed is of greater importance than a model with a very high agreement with observed data. Myers et al. (2002) compared two simple atmospheric transmission simulations: SMARTS2 (Gueymard, 2001) and SPECTRAL2 (Bird and Riordan, 1986), against a more accurate band model simulation. Myers et al. concluded that SMARTS2 was both more accurate and more adaptable than SPECTRAL2, and was the best alternative for fast simulation of the terrestrial spectral insolation.

SMARTS2 is a flexible program with the ability to accurately simulate the solar spectrum through a broad range of atmospheric conditions. However, for the purposes of optimising the optical performance of solar concentrating systems, a standard clear sky atmosphere is sufficient for most simulations (in particular, for generic simulations). In correspondence with Myers, he stated that, "SPECTRAL2 can be considered reasonably accurate where sufficient input data is lacking for the more detailed SMARTS2 approach". For these reasons and the fact that the source code for SPECTRAL2 is publicly available, it is used to generate the spectral solar distribution within the solar class.

The code SPECTRAL2 was written by Martin Rymes from the National Renewable Energy Laboratories (NREL) and is available via public FTP from NREL's website (http://www.nrel.gov/). SPECTRAL2 is a c version of the algorithm by Bird and Riordan (1986). Small modifications were made to Rymes's code: the solar position algorithm SOLPOS, a c implementation of Michalsky (1988) algorithm, was replaced with the more accurate PSA algorithm (Blanco-Muriel et al., 2001) and the variables were reallocated to fit more appropriately within the c++ class structure. However, the integrity of the code still remains and is embedded within this solar class. The default variables are described in **Table 2.**

Function	Description	Default	Units
units	Output units (1,2,3)	1	
tau500	Aerosol optical depth at 500 μm	0.27	
watvap	Perceptible water vapour	1.42	cm
alpha	Power of Angstrom	1.14	
assym	Aerosol asymmetry factor	0.65	
ozone	Ozone amount	0.34	cm
press	Air pressure	1013.25	kPa
tilt	Tilt on mirror	0.0	degrees

Table 2: Default variables for SPECTRAL2 the spectral component of the solar class *solar.h*

3. VECTOR CLASS

The second step in investigating the flux distribution in the focal plane of a concentrating system is to build a framework to simplify the projection of this solar image into this plane. Blanco-Muriel and Alarcon-Padilla (2000) summarised the seven main computer codes currently available to carry out this task.

While all of the codes mentioned by Blanco-Muriel and Alarcon-Padilla are effective at predicting the performance of solar collectors or optimising heliostat fields, all were developed at least fifteen year prior to this paper. The programs are complicated to read, are written predominantly in Fortran. Each of the codes were designed for a specific task, so converting these codes to address the performance of ones' individual concentrating system is time consuming and requires as much understanding of the code as the people who originally developed them.

The code presented in this paper does not perform an individual task nor is it immediately applicable to a particular concentrating geometry. Rather, it provides the infrastructure to build a virtual solar concentrator by using a library of simply functions. Simulations are easily comparable as the: position of the sun, the spatial and spectral energy distribution and the broadening effect of reflection, common to all implementation of concentrators are contained within one class. The users building the geometry of their solar concentrating system within the framework of the vector class can then simulate the optics of the system by tracing the generated solar image through their geometry.

3.2 Functions

The vector class builds within the frame work of a computer a 3-dimensional vector space whose basis are,

$e_i = (1,0,0)$ x-axis
$e_j = (0,1,0)$ y-axis
$e_k = (0,0,1)$ z-axis

Vectors created within this environment obey the standard laws of vector mathematics being: commutative with scalar multiplication, associative of vector addition, associative of scalar multiplication and distributive with both scaler and vector sums. The vector class facilitates these calculations. Along with these fundamental vector functions, the vector class has several other intrinsic functions that simplify the mechanics of building a ray-tracing algorithm theses are:

- Dot product
- Vector norm
- Norm square
- Reflect about a vector
- Tracing of a vector
- Rotation of a vector

- Translation of a vector

Being written in the computer language c++, the code allows the easy implementation of further functions without affecting the present code. What is presently provided is the framework of the code but much further work can be contributed to build the library into a complete set of functions representing a virtual solar collector.

4. SOLAR AND VECTOR SUMMARY

While no specific solar concentrator has been generated using the principles of these algorithms, they do allow any concentrating systems to be generated within this environment. More so, because the solar input parameters are common to any system, the solar class allows direct comparisons between different systems to be gained and detailed flux distributions in the imaging plane of concentrators to be generated. The two libraries of functions can be downloaded from http://www.physics.usyd.edu.au/~buie/ftp/

The code does not have a user-friendly front end. While this inhibits its use by those not familiar with the c/c++ computer language, it allows portability, high performance and adaptability to any concentrating system and application.

5. EXAMPLES OF APPLICATIONS AND RESULTS

Within this section a series of concentrating systems have been generated for the purpose of illustrating the versatility of the code and typical outputs that the code can generate. All of the images have been generated using MATLAB©.

5.1 Fresnel dish system

A concentrator has been constructed at the University of Sydney for testing, characterizing, and optimising solar energy conversion materials and components. The optical and heat transfer characteristics of the experimental concentrator are of great importance for the characterisation and optimisation of the solar concentrator technology used in the large-scale central receiver systems and can also assist development in any mid-to-high concentrating system.

The test facility is a 2-axis tracking parabolic Fresnel concentrator. A special consideration in this project has been the particular application of the concentrator as a test facility for solar energy conversion materials and devices. Rather than trying to maximize the total solar energy collected at the receiver, the design process has focussed on the requirements of a well-defined source of high-intensity illumination and sufficient flexibility in test parameters.

The concentrator is comprised of 18 spherical mirrors, each with an aperture area of 0.26 m^2, giving a total aperture area of 4.8 m^2. The mirrors have a radius of curvature of about 4.8 m and a rim angle of 7° (as seen from the focal point). The mirrors are bonded structures comprising an anodised aluminium reflective surface mounted on a lightweight aluminium honeycomb structure, enclosed by aluminium sheets at the back and along the sides. The reflective material is Alanod 410G with an as-new reflectivity of about 83 % quoted by the manufacturer. A hard oxide layer (~2 μm) protects the softer Aluminium surface in an outdoor environment and reduces the reflectivity deteriorating. The mirrors are attached to a 3-metre parabolic dish frame, and the focal length of the system is 2.4 m. The placement of the mirrors is 6 on an inner ring, and 12 on an outer ring.

An advantage of this set-up is that individual mirrors can be covered to provide incremental control of the solar flux up to a maximum value of about 1000 suns. Even higher concentrations are possible by employing small secondary mirrors near the primary focus of the concentrator. Uncertainties resulting from misalignment, dispersion and wavelength dependent reflection characteristics of the mirrors require that the focal area be characterised theoretically, both with respect to intensity and homogeneity. Also, the solar flux reflected from the concentrator will vary with the number of mirrors used and the time of day.

The environment of the Fresnel dish system was built within the vector class. As the optical quality of the mirror surface is relatively poor we assumed that the standard deviation of surface errors to be approximately 6 mrad. The default solar variables were accepted only that the CSR was set to 0.1, more typical for a costal city such as Sydney (Author's opinion). Figure 2 illustrates the flux distribution in the imaging plane from just one of the outer mirrors of this Fresnel dish system. The spherical aberration created from reflecting the solar image off the optical axis and onto a flat plate can clearly be seen. Also the spot size of the mirror can be accurately determined.

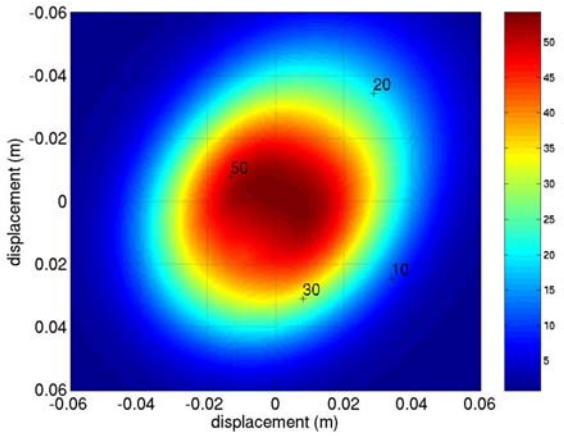

Figure 2: Theoretical concentration ratio predicted from one of the outer mirrors, (surface error 6 mrad)

Figure 3 illustrates the flux distribution in the imaging plane generated by reflecting the solar image off all 18 mirrors using the same surface error distributions.

Because of the symmetric position of the 18 mirrors the astigmatic image seen in Figure 2 is replaced by a symmetric image, with peak concentration over 1000 suns. A high flux homogenous field exists in the imaging plane with an area of approximately 0.16 m^2 assuming a zero tracking error in the parabolic collector. No experimental evidence has been collected to confirm this distribution.

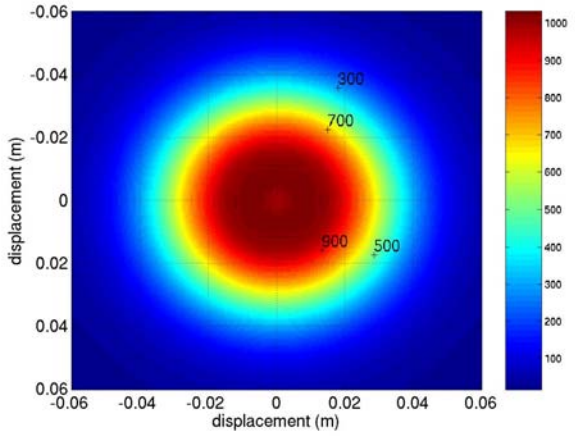

Figure 3: Theoretical concentration ratio predicted from the 18-mirror array, (surface error 6 mrad)

Using this environment, accurate flux images can be created and controlled. The desired optical characteristics can be theoretically generated and then translated to the real system.

5.2 EuroTrough

EuroTrough, created by a European consortium is a parabolic trough collector design based on the successful LS-2, LS-3 (Luz) collectors in California (Lupfert *et al*. 2000*)*. As with all linear systems, there are inherent optical losses due to the limited degrees of movement of the reflector. Using the solar and vector class, a parabolic trough collector was created whose dimensions match those of the EuroTrough.

The purpose of the model was to identify portions of the mirror module whose reflected solar radiation didn't strike the absorber line during peak fluxes. The simulations were conducted at the location of Sydney, Australia at two different times of year, summer and winter solstice.

Figure 4 illustrates the southern end of one of the mirror modules of the EuroTrough (South is positive). The red region represents a portion of the mirror whose reflected sunlight never hit the absorber line (summer or winter), the orange represents the reflector area that does not hit the absorber line during a Sydney winter and the yellow represents the distance from the end of the mirror line that continuously strikes the absorber line.

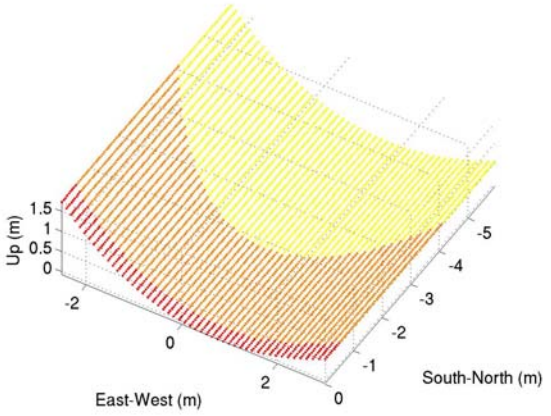

Figure 4: End losses of a parabolic collector whose dimensions match those of the EuroTrough for the location of Sydney at both Summer and Winter solstice.

The redundant aperture area relates to approximately 2.5 m^2 and 15 m^2 of aperture area respectively. This must be placed in context of the total aperture area of the modules being a redundant area of approximately 0.5% and 2.5% of the total aperture area respectively.

5.3 Central receiver system

The flux distribution in a central receiver system is extremely important for both defining the optical efficiency and determining the homogeneity of the beam. For the purpose of this simulation, a central tower receiver with a horizontal flat plate collector was generated. The absorber plane was positioned 10 m above the rotating axis of the mirrors and is centred amongst a square mirror field.

The mirror field consists of 225 closely spaced circular reflectors 2 m in diameter. Each mirror is placed on the vertices of a regular square grid 30 m by 30 m (15 by 15 array, 2 m apart). Each of the mirrors has a paraboloidal curvature with a focal length equal to the path length between its pivot point and the absorber plane. This leaves 706.9 m^2 of mirror (aperture) area.

Each mirror reflects the sun's energy to the central point in the absorber plane. A square section of the absorber 1.2 m by 1.2 m is investigated centred about the central aiming position of each of the mirror modules.

The default values for the solar class were accepted, except that instead of using a specific location a particular optical airmass was adopted. One simulation had the sun directly above the central tower or an airmass of one (sunpos(0,0)). The other considered an optical airmass of 1.5, with an azimuth angle of 0.392^c (sunpos(0.841,0.392)).

For the purpose of this paper, the flux distribution was generated either side of the focal plane. 11 slices were considered 5 above and below the focal plane in intervals of 10cm. Figure 5 illustrates all 11 slices for the AM1

simulation. The colormap has been rescales to give a greater representation of the lower flux levels.

The curves exhibit a high degree of symmetry. The focal plane (represented by a vertical displacement of 0 m) has the smallest spatial energy distribution and subsequently the highest concentration ratio. The image in the focal plane is almost spherical similar to the flux distribution in Figure 3. As you move out of the focal plane the shape of the field becomes more apparent in the flux distribution. The spatial energy distribution increases with a subsequent reduction in the concentration ratio as expected.

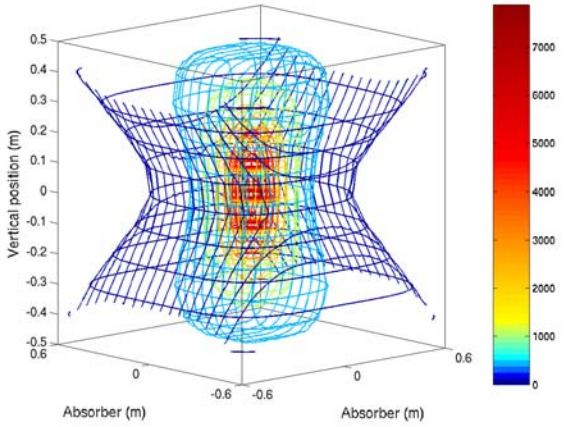

Figure 5: Flux distribution as a function of z-position through the absorber plane. (AM1) The colormap is the concentration ratio.

Figure 6 is somewhat different to Figure 5. The obvious symmetry within the image no longer exists. The concentration ratio is considerable lower primarily due to the fact that there is less that two-thirds of the energy in the focal plane (created from the cosine effect of the aperture area). The peak flux, moving out of the focal plane migrates from the central position in the image. Over time this point migrates around the central position.

This illustrates an interesting point of central receiver systems. As the solar image migrates from above the tower (AM1 to higher zenith angles) the flux distribution changes considerable out of the focal plane. This high flux region rotates about the central position during the course of the day. While the energy coming from each area of the field is similar, the flux is higher from those mirrors where the reflected image in more aligned with the optical axis of each reflector.

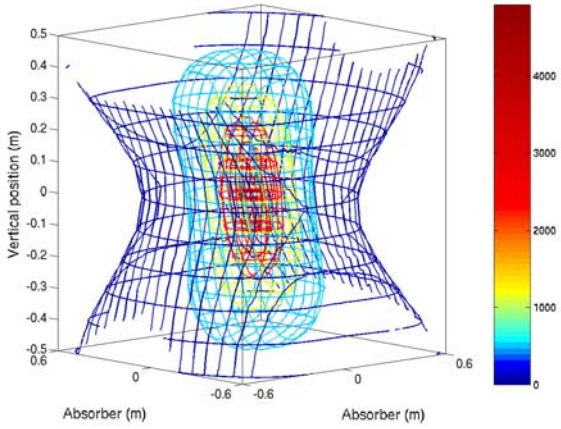

Figure 6: Flux distribution as a function of z-position through the absorber plane. (AM1.5) The colormap is the concentration ratio.

6. CONCLUSIONS

This paper provides the tools to accurately model solar concentrating systems. A class library is provided (written in the computer language c++), that contains an abstract representation of the terrestrial solar beam, including the systemic effect of reflecting that beam off a non-ideal mirrored surface. The code presented is an extension of the building blocks provided by both Blanco-Muriel et al. (2001) defining the solar position and Bird and Riordan (1986) simulating the solar spectrum. A vector class was also presented that creates the basis of Euclidean space together with functions that can facilitate a simple ray-tracing algorithm. Within this framework any optical system can be created and theoretically analysed.

While only a representative solar energy conversion systems were modelled providing little scientific value, the ease to which this methodology can be transformed to create any optical systems can be seen. No graphical user interface (GUI) is provided with this structure. The power of the code is that it is adaptable to any environment or operating system and trades the ease of use, inherent in such systems (those with a GUI) with adaptability vital for the effective comparisons and mainframe simulations. Because of the default variables, the classes have been called *The Sydney Code* (TSC 0.1)}.

REFERENCES

Bendt, P., Rabl, A., Gaul, H. W., Reed, K. A., 1979. *Optical analysis and optimization of line focus solar collectors*. Colorado, SERI/TR-34-092.

Bird, R. E., Riordan, C., (1986) Simple solar spectral model for direct and difuse irradiance of horizontal and tilted planes at the earth's surface for cloudless

atmosphere. *Journal of Climate and Applied Meteorology* 25, 87-97.

Blanco-Muriel, M., Alarcon-Padilla, D., (2000) Enertracer : A new computer tool for energy analysis of concentrating systems. *In: Proceedings of the 10th Solar PACES International Symposium on Solar Thermal Concentrating Technologies*. pp. 87-93.

Blanco-Muriel, M., Alarcon-Padilla, D. C., Lopez-Moratalla, T., Lara-Coira, M., (2001) Computing the solar vector,. *Solar Energy* 70 (5), 431-441.

Buie, D., Monger, A. G., 2001. The effect of circumsolar radiation on solar concentrating systems. *In: Proceedings of the International Solar Energy Society Solar World Conference*. Adelaide, Australia PAGE NUMBER.

Buie, D., Monger, A. G., Dey, C. J., (2002) Sunshape distributions for terrestrial solar simulations, *Solar Energy* In Press.

Lupfert *et al*. (2000*)* EuroTrough – A new parabolic collector with advanced light weight structure, *Solar Paces* 8-10 March, Sydney.

Gueymard, C., (2001) Parameterized transmittance model for direct beam and circumsolar spectral irradiance. *Solar Energy* 71 (5), 325-346.

Johnston, G., (1995) On the analysis of surface error distributions on concentrated solar collectors. *Journal of Solar Energy Engineering* 117, 294-296.

Johnston, G., (1998) Focal region measurements of the 20 m^2 tilted dish at the Australian National University. Solar Energy 63, 117-124.

Junge, C. E., (1963) *Air chemistry and radioactivity*. Academic Press, New York.

Michalsky, J. J., (1988) The Astronomical Almanac's algorithm for approximate solar position (1950-2050). *Solar Energy* 40 (3), 227-235.

Mie, G., (1908) Beitrage zur optik truber medien, speziell kolliodaler metallosungen. Ann. Physik 25, 377-445.

Myers, D. R., Emery, K., Gueymard, C., (2002) Terrestrial solar spectral modeling tools and applications for photovoltaic devices. *In: Proceedings of the 29th IEEE Photovoltaic Specialists Conference*. May New Orleans, LA, Institute of Electrical and Electronics Engineers, pp. 1683-1686.

Neumann, A., Witzke, A., Jones, S. A., Schmitt, G., (2002) Representative terrestrial solar brightness profiles. *Journal of Solar Energy Engineering,* 124, 198-204.

Noring, J. E., Grether, D. F., Hunt, A. J., (1991) Circumsolar Radiation Data: The Lawrence Berkeley Laboratory Reduced Data Base. In*: National Renewable Energy Laboratory*. December, NREL/TP-262-4429. URL http://rredc.nrel.gov/solar/pubs/circumsolar/title.html

Rabl, A., (1985) *Active Solar Collectors and Their Applications*. Oxford University Press.

Walraven, R., (1978) Calculating the position of the sun. *Solar Energy* 20 (5), 393-397.

Walraven, R., (1979). Erratum. *Solar Energy* 22, 195.